Progress in Oceanography 174 (2019) 131–142

Contents lists available at ScienceDirect

Progress in Oceanography

journal homepage: www.elsevier.com/locate/pocean

Hydrographic variability along the inner and mid-shelf region of the western Ross Sea obtained using instrumented seals

Andrea Piñones[a,b,c,*], Eileen E. Hofmann[d], Daniel P. Costa[e], Kimberly Goetz[f], Jennifer M. Burns[g], Fabien Roquet[h], Michael S. Dinniman[d], John M. Klinck[d]

[a] Instituto de Ciencias Marinas y Limnológicas, Universidad Austral de Chile, Valdivia, Chile
[b] Centro FONDAP de Investigación en Dinámica de Ecosistemas Marinos de Altas Latitudes (IDEAL), Universidad Austral de Chile, Valdivia, Chile
[c] Centro de Investigación Oceanográfica COPAS Sur-Austral, Universidad de Concepción, Concepción, Chile
[d] Center for Coastal Physical Oceanography, Old Dominion University, Norfolk, VA, USA
[e] Department of Ecology and Evolutionary Biology, University of California, Santa Cruz, CA, USA
[f] National Institute of Water and Atmospheric Research (NIWA), New Zealand
[g] Department of Biological Sciences, University of Alaska, Anchorage, AK, USA
[h] Department of Marine Sciences, University of Gothenburg, Gothenburg, Sweden

ARTICLE INFO

Keywords:
Ross Sea
Seal satellite tags
Wind variability
Density gradients
Heat content

ABSTRACT

Temperature and salinity measurements obtained from sensors deployed on Weddell seals (*Leptonychotes weddellii*) between late austral summer and the following spring for 2010–2012 were used to describe the temporal and spatial variability of hydrographic conditions in the western Ross Sea, with particular emphasis on the inner-shelf region off Victoria Land and McMurdo Sound. Potential temperature-salinity diagrams constructed for regions where the seals remained for extended periods showed four water masses on the continental shelf: Modified Circumpolar Deep Water, Antarctic Surface Water, Shelf Water and Modified Shelf Water. Depth-time distributions of potential density and buoyancy frequency showed the erosion of the upper water column stratification associated with the transition from summer to fall/winter conditions. The within-year and inter-annual variability associated with this transition was related to wind speed. Changes in upper water column density were positively correlated with cross-shelf wind speeds $> 5.5\ m\ s^{-1}$ with a 3–4 day lag. A range of wind speeds was required to erode the density structure because of different levels of stratification in each year. A comparison of wind mixing potential versus stratification (Wedderburn number) showed that synoptic scale wind events during 2012 with speeds of 5.5 and $6.5\ m\ s^{-1}$ were needed to erode the summer stratification for Ross Island and Victoria Land regions, respectively. Stronger winds ($> 8.5\ m\ s^{-1}$) were required during 2010 and 2011. The interannual variability in total heat content accumulated during summer (about 20%) was related to the duration of open water, with the largest heat content occurring in 2012, which was characterized by a summer sea ice minimum stronger than other years and relatively higher mCDW influence over the mid and outer-shelf regions. The heat content was lost after mid-April and reached a minimum in winter as a result of deep winter convection. The quantitative analysis of hydrographic variability of the inner-shelf region of the western Ross Sea obtained from the seal-derived measurements provides a baseline for assessing future changes.

1. Introduction

The Antarctic continental slope and shelf are regions where traditional shipboard, short-term mooring, satellite, and Argo float coverage is limited or absent due to relatively heavy ice cover. As a result, understanding of basic hydrographic properties, such as the seasonal progression of the thermohaline structure and heat content variability of the upper ocean mixed layer, is limited. The advent of small electronic tags and associated sensors that can be placed on a variety of marine animals provided an approach for obtaining physical oceanographic data from areas that are difficult or even impossible to sample (Charrassin et al., 2008; Roquet et al., 2009, 2013; Fedak, 2013). These instruments also provided increased understanding of animal movement patterns and habitat use (Bost et al., 2009, 2015; Costa et al., 2012).

Conductivity-temperature-depth satellite data relay loggers (CTD-

* Corresponding author at: Instituto de Ciencias Marinas y Limnológicas, Universidad Austral de Chile, Valdivia, Chile.
E-mail address: andrea.pinones@uach.cl (A. Piñones).

https://doi.org/10.1016/j.pocean.2019.01.003

Available online 06 January 2019

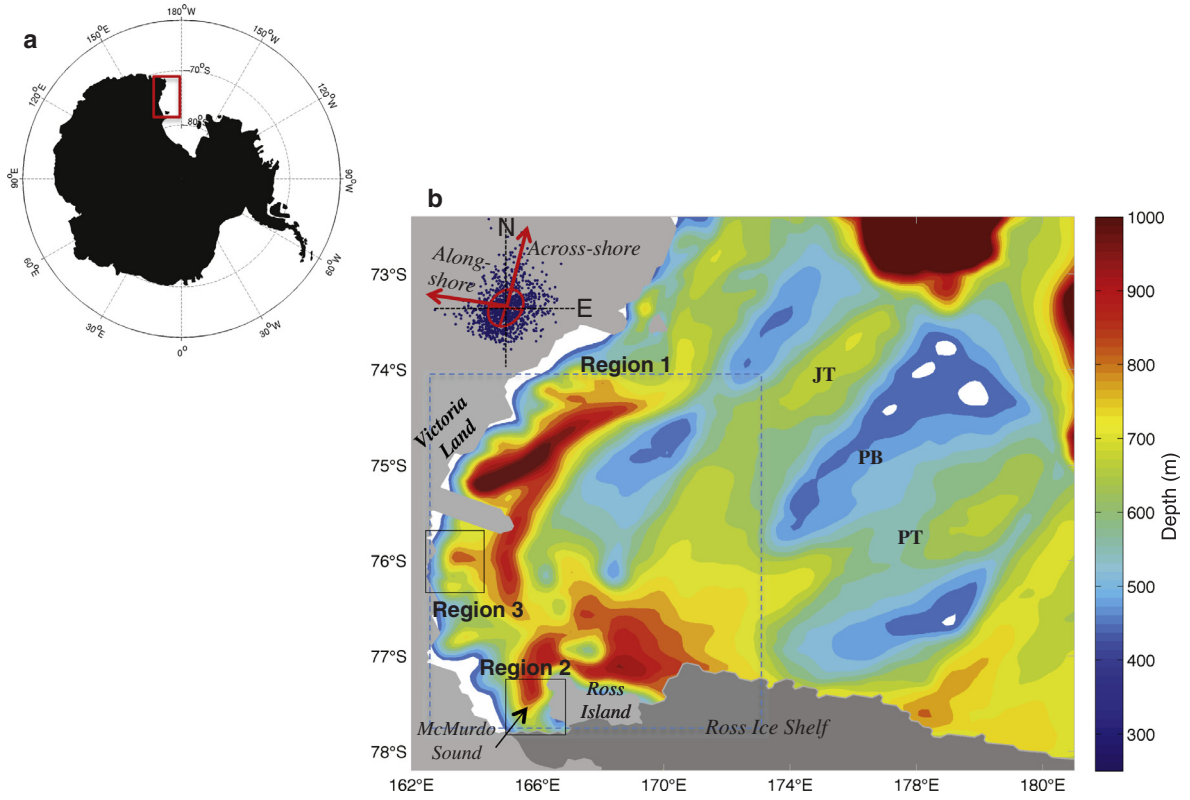

Fig. 1. (a) Map of Antarctica showing the location of the western Ross Sea (red box). (b) Region 1 (dashed box) indicates the larger area that was sampled by the seals. The areas around Ross Island (Region 2, solid line box) and off Victoria Land (Region 3, solid line box) included extensive sampling by seals. The inset plot (upper left) shows the rotated maximum axis of variability (red arrows) for the wind data (blue dots) near Ross Island. The across-shore wind component is positive offshore; the along-shore wind component is positive from the eastern to the western Ross Sea. The Ross Ice Shelf is indicated and bathymetry (m) is shown. Geographic features are indicated as: Pennell Bank – PB, Pennell Trough – PT, Joides Trough – JT. (For interpretation of the references to colour in this figure legend, the reader is referred to the web version of this article.)

SDRL) deployed on animals that dive, such as seals, offer a significant advantage in that they provide vertical profiles of temperature and salinity (Biuw et al., 2007) over regional scales, as well as repeated profiles that provide localized time series (Costa et al., 2008). Several species of seals are residents of Antarctic shelf and slope regions for some or all the year, and as such provide opportunities for collection of hydrographic data that otherwise would be unavailable (Costa et al., 2008; Roquet et al., 2013).

The Ross Sea (Fig. 1) overlies the largest continental shelf in the Southern Ocean and is one of a few locations that forms and exports Antarctic Bottom Water (Orsi et al., 1999; Gordon et al., 2009, 2015; Budillon et al., 2011). The Ross Sea is experiencing increased sea ice extent (Comiso et al., 2011), decreased duration of the summer ice-free period (Parkinson, 2002; Stammerjohn et al., 2008, 2011), decreased sea surface temperature (Comiso, 2010, Comiso et al., 2017), and stronger southerly winds (Turner et al., 2009, 2016; Holland and Kwok, 2012); all of which affect the upper ocean thermohaline properties. Understanding of Ross Sea water masses, thermohaline properties, and hydrographic variability is derived mostly from summer measurements during ice-free conditions. The changes in the upper ocean thermohaline properties in winter, which set up conditions that influence subsequent sea ice cover and water mass formation, are poorly understood and resolved in Ross Sea hydrographic measurements.

Weddell seals (*Leptonychotes weddellii*) are the southernmost occurring seal species and are residents of the high latitudes in the Ross Sea, extending throughout the inner-shelf fast ice and pack ice regions over the continental shelf (Castellini et al., 1992; Testa, 1994; Burns et al., 1999; Burns and Kooyman, 2001). Weddell seals have high site fidelity (Testa, 1994), which supports a consistent sampling region. Weddell seals are capable of long (> 60 min) and deep (> 600 m) dives, but most of their diving activity is focused at midwater depths of 150–300 m during summer, although benthic dives are common in winter months (Castellini et al., 1992; Testa, 1994; Burns et al., 1999; Goetz, 2015). As a result, Weddell seals provide vertical profiles that capture the upper ocean variability and multiple dives in the same region provide time series that allow the seasonal progression of this variability to be characterized and compared. Thus, this species can provide extensive coverage of specific regions of the Ross Sea.

As part of a study of predator winter foraging behavior and habitat utilization in the Ross Sea, CTD-SRDL tags were deployed on Weddell seals in and around McMurdo Sound in the southwestern Ross Sea from 2010 to 2012 (Goetz, 2015). The tagging in January and February followed completion of summer molting, coincided with fall foraging, and extended through the winter into the following spring (Goetz, 2015).

Seasonal changes in the upper ocean thermohaline characteristics result from interactions of complex dynamical processes. The summer upper ocean in the Ross Sea is stratified by heating from solar radiation and melting of sea ice (Fig. 2). During the fall/winter transition this stratification is eroded by wind mixing and heat loss to the atmosphere. The fall/winter cooling sets up formation of sea ice that leads to brine rejection and deep water convection, which also erodes summer stratification. In the mid and outer-shelf regions intrusions of modified Circumpolar Deep Water (mCDW) provide heat and salt, which are exchanged with the upper water column (Fig. 2). The objective of this study was to resolve the spatial and temporal variability associated with this summer to fall/winter transition using three years of measurements provided by tagged Weddell seals, allowing quantitative assessment of processes affecting seasonal and interannual variability in the thermohaline properties of the upper ocean in the southwestern Ross Sea.

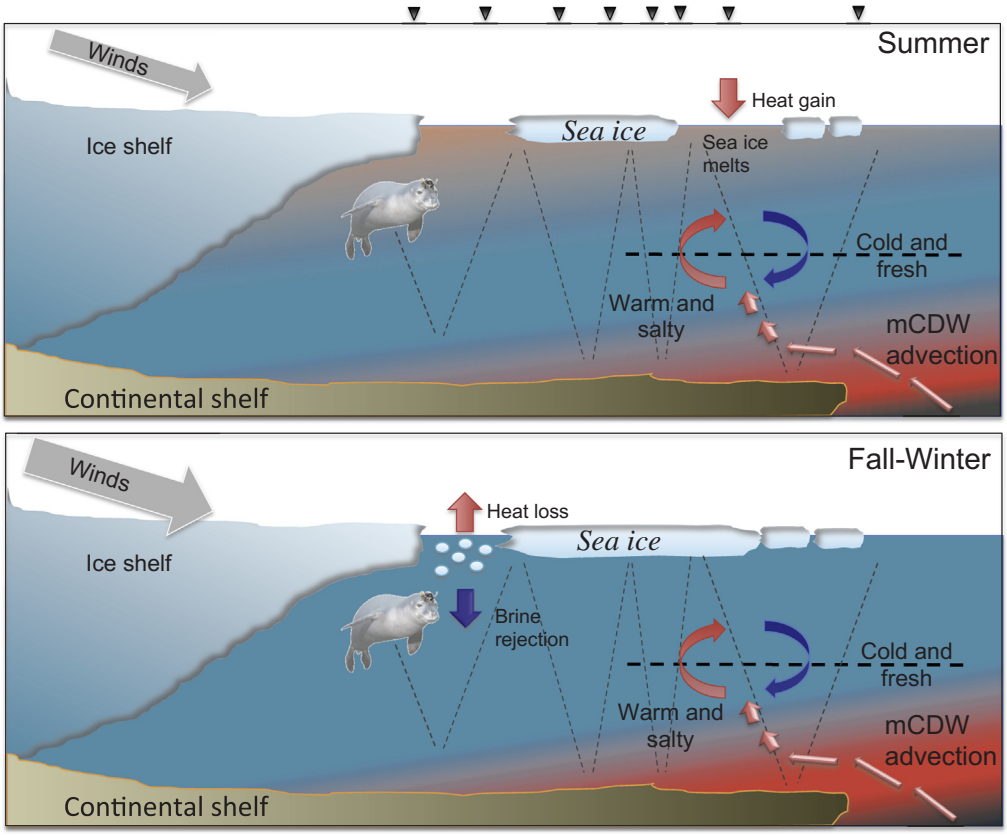

Fig. 2. Conceptual diagram of the dynamical processes occurring in the upper ocean on the Ross Sea continental shelf in summer (upper panel) and fall/winter (lower panel). The summer to fall/winter transition is characterized by changes in sea ice distribution, and upper ocean stratification and heat content. The presence of modified Circumpolar Deep Water at depth provides heat and salt to the subsurface layers of the mid and outer Ross Sea continental shelf. External forcing is provided by solar radiation and winds. Tagged Weddell seals transit the water column (triangles denote seal dive locations) in summer and fall/winter measuring the temperature and salinity of the upper water column, capturing the changes in water column properties.

2. Methods

2.1. Seal tags

Between February to November 2010, January to October 2011, and February to November 2012 a total of 68 CTD-SRDL tags were deployed on Weddell seals in the southwestern Ross Sea (Table S1, supplementary material), The time gaps at the start of the austral summer and at the end of the year are from completion of molting and sensor loss due to molting, respectively. The precision of the conductivity, temperature and pressure (depth) sensors is ± 0.003 $mS\,cm^{-1}$, ± 0.001 °C, and ± 5 dBar, respectively. The tags were optimized to collect oceanographic data relative to seal ascent speeds (~1 $m\,s^{-1}$). The CTD data were collected at 0.5 Hz. Prior to ARGOS transmission, the dive profiles were summarized into 20 points including 10 fixed pressures adaptively selected based on the maximum pressure of the dive, and augmented by 10 points selected by a broken-stick algorithm (Rual, 1996; Fedak et al., 2001, 2002; Boehme et al., 2009). A pseudo-random method was used to transmit an unbiased sample of stored records. The tags were calibrated prior to deployment and comply with ITS-90 (International Temperature Scale 1990) and PSS-78 (Practical Salinity Scale 1978) specifications. Additional details of seal tagging procedures were provided by Goetz (2015).

2.2. Temperature and salinity data

The tagged seals moved throughout the western region of the Ross Sea (Region 1, Fig. 1). The location estimates for individual seals were adjusted for accuracy as described in (Roquet et al., 2014). The adjusted CTD data have an estimated accuracy of 0.02 °C in temperature and 0.05 in salinity (Roquet et al., 2011, 2014). For this analysis, the areas where the dive data were concentrated were binned into 10 km × 10 km cells and the number of dives that provided temperature and salinity vertical profiles was tallied (Fig. 3), similar to the approach used by Costa et al. (2008). More than 79% of seal dives that returned temperature and salinity data were from the inner-mid shelf region between Victoria Land and around Ross Island (Fig. 3); regions that were consistently sampled in all three years. The temperature and salinity measurements in the three regions covered by the seals (identified on Fig. 1) were binned at 10-m (from 0 to 200 m) and 20-m (from 200 to 400 m) and 1-day intervals and an average calculated for each bin (Fig. 3).

The data from Region 1 (inner-mid shelf, Fig. 1) were used to construct potential temperature-salinity diagrams (Fig. 4), across-shelf temperature distributions (Fig. 5), and time-depth distributions of density (Fig. 6a). Buoyancy frequency (Fig. 6b) for 2010, 2011, and 2012 was calculated as:

$$N^2 = -\frac{g}{\rho}\frac{\partial \rho}{\partial z} \quad (1)$$

where g is gravity (9.8 $m^2\,s^{-1}$) and $\partial\rho/\partial z$is the change in potential density (ρ) with depth (z). Time-depth distributions of density were also calculated for Region 2 (Fig. 7a–c, Ross Island) and Region 3 (Fig. 7g–i, Victoria Land). For the time-depth distributions, gaps of 3 days or less in the seal dive data were filled by linear interpolation.

2.3. Wind and sea ice fraction distributions

Winds for the Ross Sea region for 2010–2012 were obtained from the ERA-Interim reanalysis dataset (Dee et al., 2011). Winds were extracted from the two grid points closest to Victoria Land and Ross Island at 6-hour intervals and daily averages were calculated. The daily winds were rotated to the major axis of variability, which corresponded to the across-shore direction. After rotation, the main axis of variability corresponded to winds blowing from land to over the ocean, i.e. positive offshor, and the minor variability axis corresponded to winds blowing along the shore, positive from the eastern to the western side in the case of Ross Island (see inset Fig. 1b) and positive from southern to the

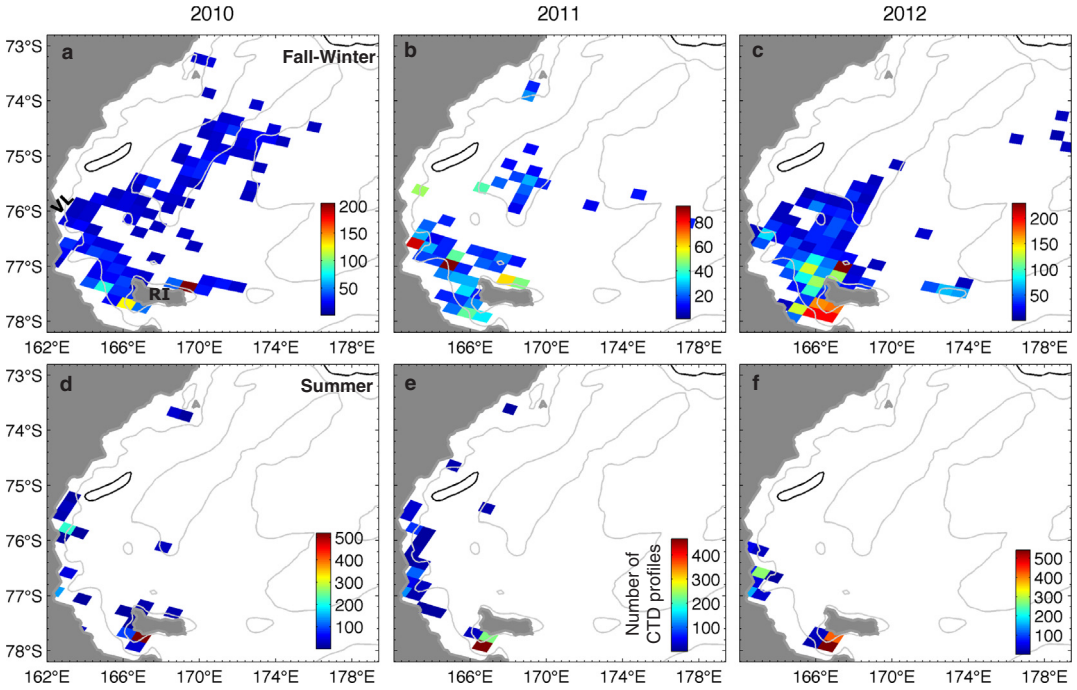

Fig. 3. The total number of CTD vertical profiles obtained from the tagged seals in 10 km × 10 km bins in each year (2010–2012) for (a–c) Fall-Winter (15 March–15 September) and (d–f) Summer (January–15 March). Only regions with 10 or more available CTD profiles per unit area are shown (color scale). The 500-m and 1000-m isobaths are shown (grey and black contours, respectively). (For interpretation of the references to colour in this figure legend, the reader is referred to the web version of this article.)

northern side in the case of Victoria Land. Time series of the across and along-shore wind components were then constructed for an area in the southwestern Ross Sea (Fig. 6c) consistent with box 1 (Fig. 1) and for Ross Island (Fig. 7d–f) and Victoria Land (Fig. 7j–l).

Daily sea ice fraction time series for the Ross Island (Region 2) and Victoria Land (Region 3) regions for 2010, 2011 and 2012 were obtained from the NOAA/National Snow and Ice Data Center Climate Data Record of passive microwave sea ice distributions. These time series were smoothed using a triangular moving average filter to remove high frequencies (< 3 days).

2.4. Analysis methods

Cross-correlations and coherence and phase spectra (Emery and Thomson, 1998) were used to determine relationships between wind and water column vertical density structure. Coherence or cross-spectral analysis identifies signals in different time series with similar spectral frequency bands. The phase lag provides information about the timing of one spectral signal relative to the other. Cross-correlations were estimated between the daily-averaged across-shore wind component and water column density (from surface to 300 m). Coherence

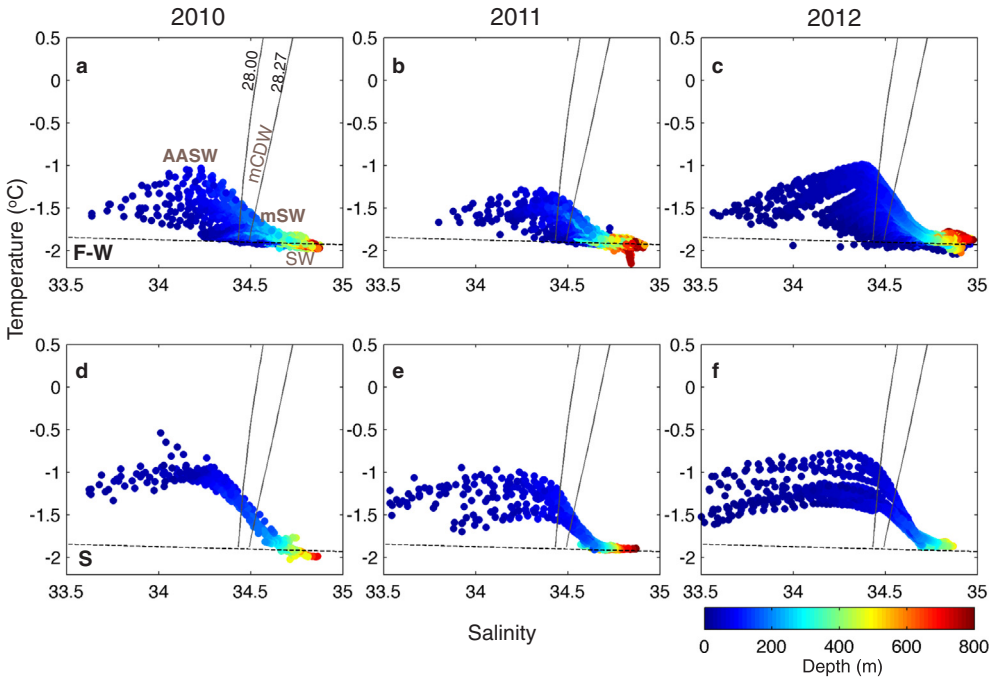

Fig. 4. Salinity and potential temperature diagrams constructed from the seal-derived CTD measurements for (a–c) fall-winter (F-W) and (d–f) summer (S) for the inner-mid shelf region for 2010, 2011 and 2012. The depth (m) of the temperature-salinity measurements is shown by the color scale. The main water masses observed in the study region are indicated as: Antarctic Surface Water (AASW), modified Circumpolar Water (mCDW), modified Shelf Water (mSW) and Shelf Water (SW). Neutral density contours (28.00 and 28.27 kg m^{-3}) and the freezing point (dotted line) are indicated. (For interpretation of the references to colour in this figure legend, the reader is referred to the web version of this article.)

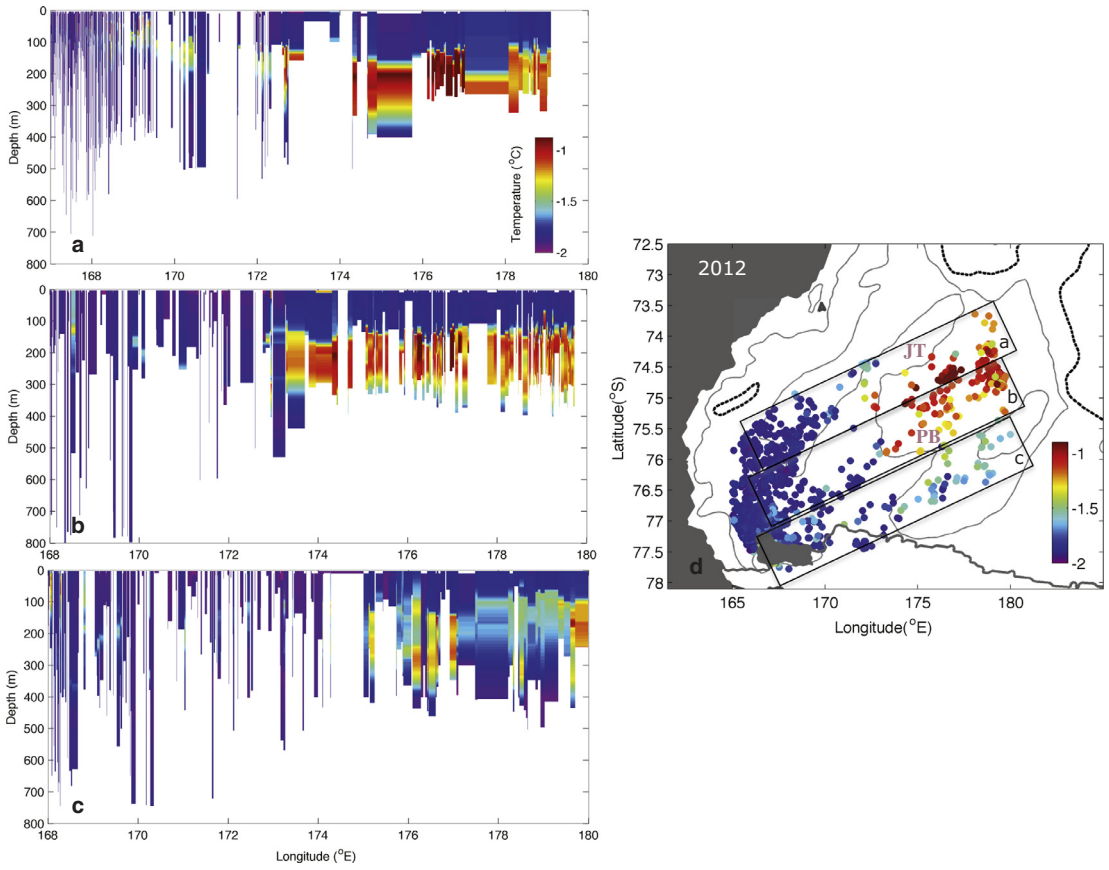

Fig. 5. (a–c) Depth-longitude sections of temperature (°C) from the inner- to the mid-shelf constructed from seal-derived measurements in winter 2012. (d) Spatial distribution of temperature at 200 m for the regions shown in a–c, references are shown in the bottom right corner of the section. The three regions cover the Joides Trough (JT) and Pennell Bank (PB) and extend to the inner shelf near Ross Island. This year the seals dived farther offshore. The 500-m and 1000-m isobaths are shown (grey and black contours, respectively).

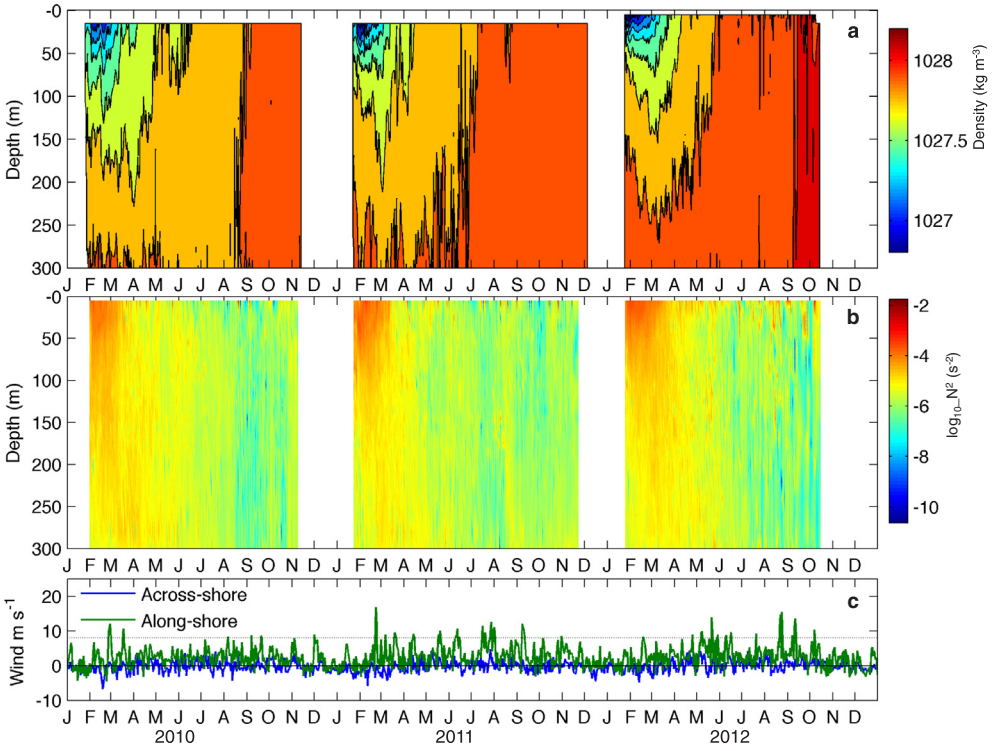

Fig. 6. (a) Composite time-depth distributions of density (kg m^{-3}) and (b) buoyancy frequency (s^{-2}) constructed using the seal-derived CTD measurements from the inner-mid shelf region from February to November 2010 (left panels), January to October 2011 (middle panels) and February to November 2012 (right panels). (c) Time series of rotated across-shore and along-shore wind speed (m s^{-1}) derived from the ERA-Interim reanalysis dataset for 2010–2012 with wind pulses > 8 m s^{-1} indicated (dashed line) for a region between Ross Island and Victoria Land.

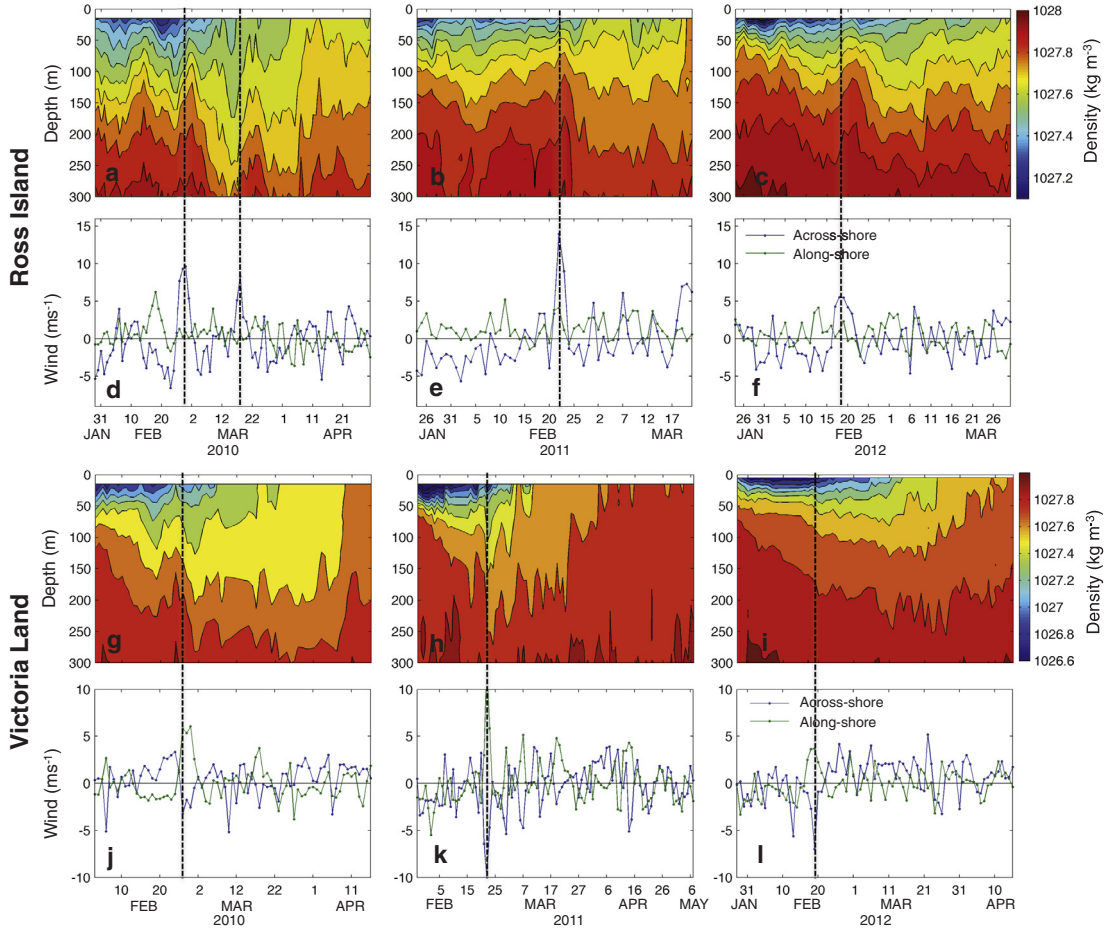

Fig. 7. Time-depth distributions of density (kg m^{-3}) from the seal-derived CTD measurements for the Ross Island (a–c) and Victoria Land (g-i) regions for austral summer-fall of 2010 (left panels), 2011 (middle panels), and 2012 (right panels). Time series of rotated across-shore and alongshore wind speed (m s^{-1}) derived from the ERA-Interim reanalysis dataset for Ross Island (d–f) and Victoria Land (j–k). Periods of maximum wind speed are indicated (vertical dashed lines).

spectra between wind and water column density and across- and alongshore wind and water column density were estimated for Regions 2 and 3 at a range of depths (5, 50, 100, 200, 400 m) using 10 degrees of freedom (Fig. 9a, c, e). The phase lag (days) was estimated for each depth and year and values for coherences above the significance level of 90% were retained (Fig. 9b, d, f).

The interaction of wind events with summer stratification was quantified using the Wedderburn number (W) (Fig. 10), which provides a measure of mixed layer stability ($W > 1$) or instability ($W < 1$) based on the balance between wind forcing and the pycnocline tilt (Imberger, 1985), and is calculated as:

$$W = (g'h^2)/(u_*^2 L) \quad (2)$$

where $g' = g\Delta\rho/\rho$ is the reduced gravity due to a vertical density gradient $\Delta\rho$, h is depth of the summer mixed layer, $u_* = \sqrt{\tau/\rho}$ is the surface shear velocity due to wind stress (τ) and L is the length of the inner-shelf area in the direction of the wind (L = 40 km, determined by size of subregions 2 and 3, Fig. 3). Wind stress was estimated from the winds using a drag coefficient of 1.3×10^{-3} and air density of 1.2 kg m^{-3}. The seasonal mixed layer depth (h) was estimated using a density threshold defined by the shallowest depth at which density differed from the value at 15 m by 0.01 kg m^{-3} (Smith et al., 2011; Kaufman et al., 2014).

2.5. Heat content estimates

The total heat content (HC) of the upper ocean was estimated from the time-depth distributions of potential temperature (θ) (Fig. 11). The heat content was calculated relative to the surface freezing temperature ($T_f = -1.9$ °C) at a salinity of 34.5 and surface pressure (0 dbar) as:

$$HC = \int_0^{zp} \rho c_p(\theta - T_f)dz \quad (3)$$

where zp is the depth of integration (300 m), ρ is density of seawater and c_p is the specific heat of seawater (3994.6 J °C^{-1} kg^{-1}).

3. Results

3.1. Temperature-salinity distributions

The seasonal progression in temperature and salinity from fall-winter (Fig. 4a, b, c) to summer (Fig. 4d, e, f) in Region 1 indicated in potential temperature-salinity (T-S) diagrams shows the water masses expected for this part of the continental shelf but also shows the interannual variability in the properties of the water masses. The fall-winter seal observations were primarily from the inner and mid-shelf regions; summer observations were from the inner shelf (Fig. 3). The seals provided few observations from the outer shelf (Fig. 3, Table 1). Antarctic Surface Water (AASW), characterized by low salinities (~34), cold temperatures (−0.5 °C to −1.6 °C), and neutral density (γ^n) less than 28 kg m^{-3}, was present in the upper water column in each season and year. Below AASW and above modified shelf water (mSW, $\theta > -1.85$ °C, $\gamma^n > 28.27$) was mCDW (> 34.4, −1.5 to 0.5 °C, $28 < \gamma^n < 28.27$). The winter T-S distributions show mSW and Shelf Water (SW, $\theta < -1.85$ °C, $\gamma^n > 28.27$) in all years (Fig. 4a, b, c). The

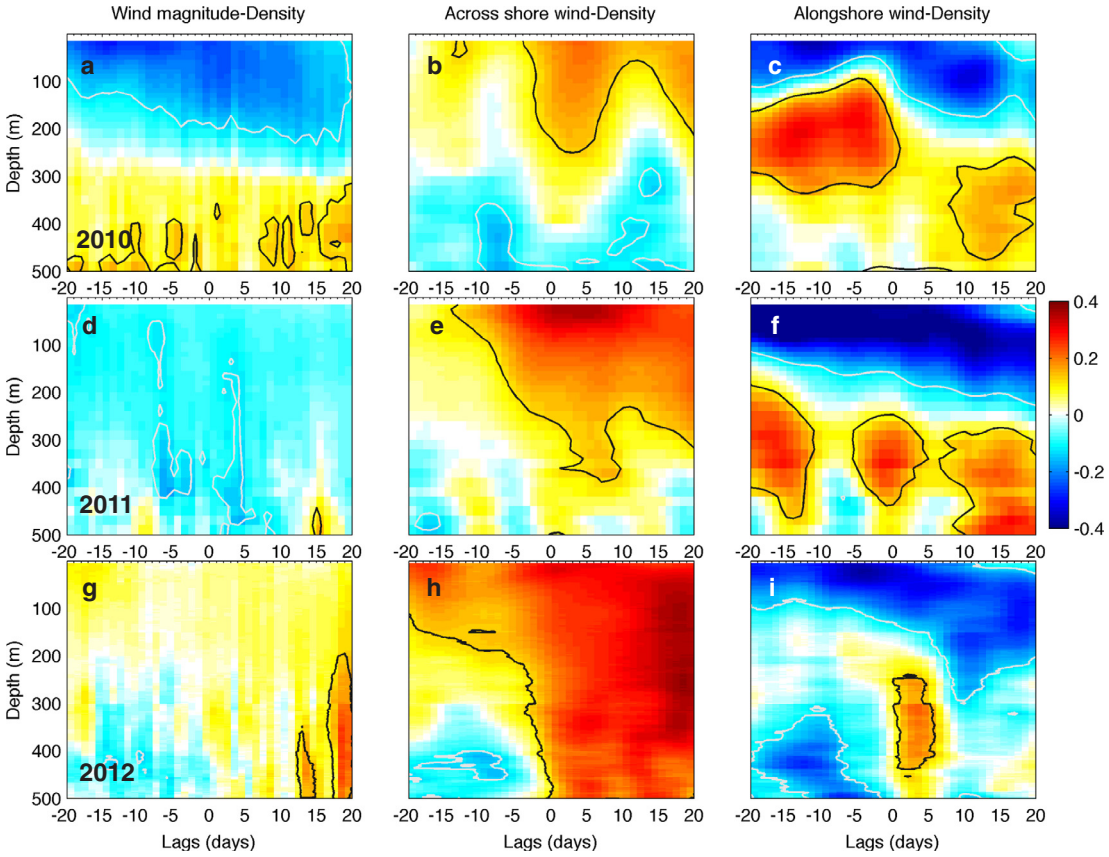

Fig. 8. Lagged cross-correlation (in days) by depth between wind magnitude and density (a, d, g), across-shore wind and density (b, e, h), alongshore wind and density (c, f, i) for 2010, 2011 and 2012. Positive (negative) correlations are indicated by warm (cool) colors. The 95% significance levels for positive (black lines) and negative (white lines) correlations are indicated.

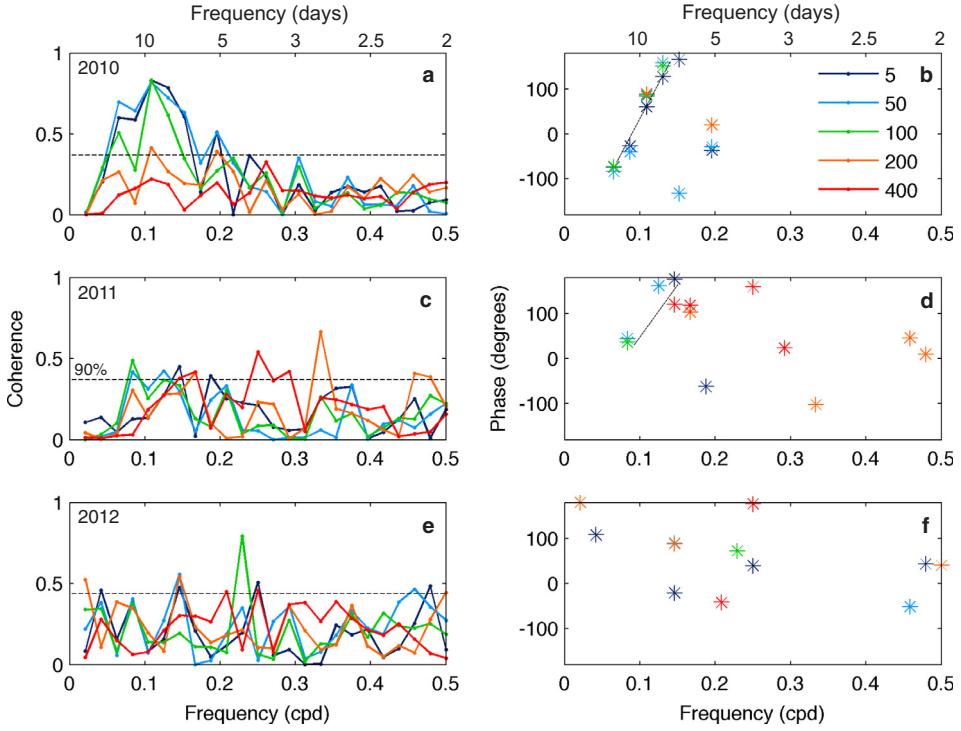

Fig. 9. Coherence (a, c, e) and phase (b, d, f) spectra calculated for across-shore wind and water density at five depths in the Victoria Land region for 2010 (a, b), 2011 (c, d) and 2012 (e, f). Dashed line represents the significance level of 90%.

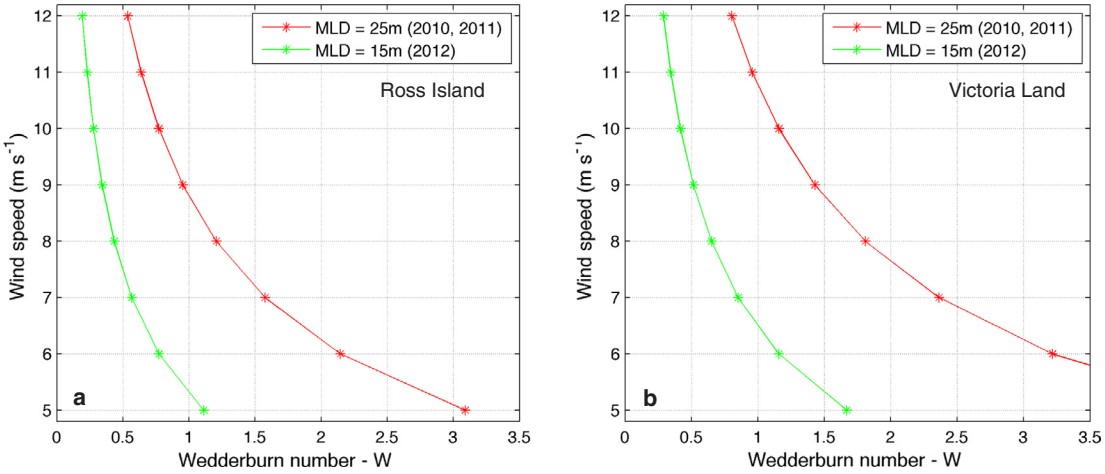

Fig. 10. Wedderburn number estimated for (a) Ross Island and (b) Victoria Land for two mixed layer depths (MLD).

depth associated with mSW is in the range of 200–300 m and that for SW is in the range of 500–800 m (Fig. 4).

The summer seal observations show the same four water masses (Fig. 4d, e, f). The signature of AASW was fresher (< 34) and colder in 2011. In all years, mSW was present and SW was seen in 2010 (Fig. 4d, e, f). The seasonal formation and erosion of AASW from fall-winter 2011 to summer 2011 produced two branches with differing characteristics which persisted into 2012.

The mid-shelf was mostly occupied by mCDW, which was well defined in the three years (Figs. 4 and 5). Across-shelf temperature sections that extend from the inner continental shelf offshore along Joides Trough (Fig. 5a) and Pennell Bank (Fig. 5b) show the extension of mCDW (> −1.3 °C, salinity 34.6 Fig. S1) from the outer shelf onto the mid-shelf. The signature of this water mass is eroded towards the inner shelf where AASW (> −1.6 °C) is observed throughout the water column. At 200 m mCDW (> −1 °C, salinity 34.6 Fig. S1) is present over Pennell Bank and its signature is eroded inshore, consistent with the across-shelf temperature sections (Fig. 5c). This water mass floods the continental shelf below 200 m over Pennell Bank (Fig. 5c).

Table 1
Summary of the CTD profiles obtained from tagged Weddell seals for the inner-mid shelf region, outer shelf region, Ross Island and Victoria Land in 2010, 2011 and 2012. The CTD profiles are separated into summer (1 January–15 March) and fall-winter (16 March–15 September) periods.

Region	2010	2011	2012
Inner-mid shelf			
Summer	1739	1508	1871
Fall-Winter	2410	2503	3354
Outer shelf			
Summer	90	59	27
Fall-Winter	1105	558	348
Ross Island			
Summer	458	493	715
Fall-Winter	204	676	223
Victoria Land			
Summer	932	703	1050
Fall-Winter	1230	633	1139

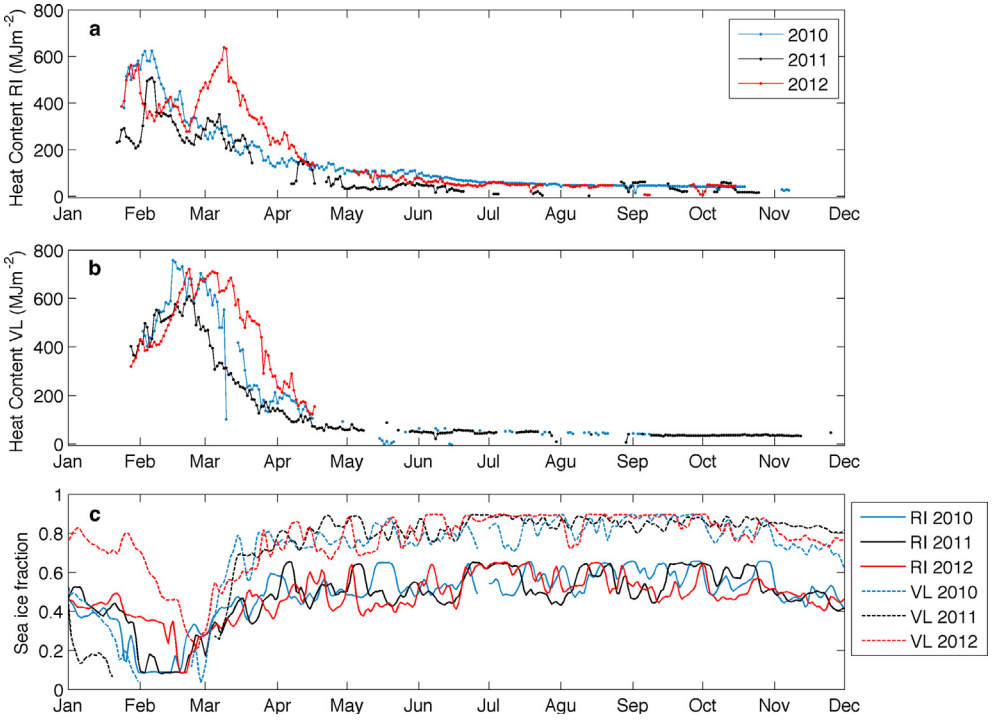

Fig. 11. Total heat content of upper 300 m calculated for the (a) Ross Island (RI) and (b) Victoria Land (VL) regions for 2010 (blue), 2011 (black) and 2012 (red) from the seal-derived temperature data. Sea ice fraction was obtained from Special Sensor Microwave Imager measurements, which provide daily sea ice for January 2010 to December 2012. (For interpretation of the references to colour in this figure legend, the reader is referred to the web version of this article.)

The horizontal distribution of temperature at 200 m constructed from individual seal dives provides a view of the spatial variability of mCDW in the western Ross Sea (Fig. 5d). This water mass moves onto the continental shelf around Joides Trough and Pennell Bank and extends to the mid-shelf region.

3.2. Water column characteristics in the inner and mid shelf regions

The time-depth distributions of density in the inner-mid shelf region show the progression from a stratified to a well-mixed water column, starting in mid-summer (February) and continuing into spring (end of November) (Fig. 6a). Surface densities remain low ($< 1027.3\,kg\,m^{-3}$) until the end of March-early April (early winter) in each of the three years. Densities greater than $1027.7\,kg\,m^{-3}$ occurred throughout the upper 300 m in August 2010 and June 2011 and 2012. Densities in excess of $1028\,kg\,m^{-3}$ occurred in September and October 2012. The only modification to this pattern was associated with high frequency variability that occurred in the upper water column (< 50 m) in August to September of 2012 (late winter).

The time-depth distributions of buoyancy frequency show that values of order $\sim 10^{-4}\,s^{-2}$ (i.e. $\log_{10}(N^2) \approx -4$) were frequent during all years and observed in the upper 50 m consistently until the end of February in 2010 and 2011 and until mid-March in 2012 (Fig. 6b). The buoyancy frequencies during winter were one order of magnitude less than during summer ($2 \times 10^{-5}\,s^{-2}$ or $\log_{10}(N^2) \approx -8$). At depth, the strong surface stratification disappeared below ~ 150 m (Fig. 6b).

The temporal variability of wind conditions over the inner-mid shelf region showed wind pulses in excess of $10\,ms^{-1}$ during all years, but more pulses were observed during 2011 and 2012. Larger pulses observed between August and September 2012 were consistent with high frequency variability that occurred in the upper water column (Fig. 6c).

The time-depth distributions of density constructed for the Ross Island (Fig. 7a, b, c) and Victoria Land (Fig. 7g, h, i) regions in each year show the presence of less dense water at the surface in summer, as expected, and the erosion of this layer into fall. However, the pattern of density progression varies between the two regions. The near surface vertical density gradient in the Ross Island region persisted until the end of February during 2010 and 2011, and until mid-March during 2012. The vertical density gradient in the surface layer (< 50 m) in the Victoria Land region showed a similar pattern, was largely eroded by late February in 2010 and 2011, and also persisted until mid-March in 2012. The vertical density gradient over the top 300 m at Ross Island is eroded by mid-March during 2010 and 2012, and by late February in 2011. The vertical density gradient was stronger in Victoria Land (Fig. 7g, h, i), as a result of a shallow and fresh surface mixed layer that extended to 25–35 m. The pycnocline was deeper during 2010 and 2011 (~ 60 m) and shallower during 2012 (~ 40 m); stronger vertical gradients were observed for 2011 and 2102. The vertical gradient over the entire 300 m is generally much weaker by April in Victoria Land compared to Ross Island.

3.3. Relationship with wind conditions

The across-shore wind (rotated U-component, positive offshore, see Fig. 1) during summer at Ross Island (Fig. 7d, e, f) and Victoria Land (Fig. 7j, k, l) was stronger in 2010 and 2011 than in 2012. The across-shore wind in the Ross Island region was dominated by pulses of 3–6-day duration at 12–22-day intervals (Fig. 7d, e, f). The strongest wind pulses occurred in February 2010 and 2011. In 2012, the wind pulses were reduced in intensity during the transition from fall to winter (Fig. 7f). The strong off-shore wind pulses ($> 8\,m\,s^{-1}$) observed in summer 2010 and 2011 in the Ross Island region (Fig. 7d, e) produced upwelling favorable conditions and coincided with the rise of the isopycnals (Fig. 7a, b, c). Winds with speeds of about $5\,m\,s^{-1}$ (directed offshore) also occurred and coincided with deepening of the isopycnals and downward mixing of lower density surface waters. The frequency and timing of the across-shore wind pulses in the Victoria Land region were similar, but the strongest wind events (Fig. 7j, k, l) were on-shore (negative direction) and associated with deepening of the isopycnals below 50 m, which mixes low-density surface waters deeper in the water column (Fig. 7g, h, i).

The relationship between wind events and the erosion of summer stratification was investigated further by calculating cross-correlations between wind and density at depth for the inner-mid shelf region in the three years (Fig. 8). For 2010, significant negative correlations obtained in the upper 200 m associated stronger winds with a decrease in surface density; positive correlations were associated with a density increase below 400 m (Fig. 8a). During 2011 the same pattern was observed below 100 m with an increase in wind magnitude leading by 4–5 days a decrease in subsurface density and an increase in density at 500 m 15 days later (Fig. 8d). During 2012 this pattern was observed only at depth with the increase in wind magnitude leading by 15 and 20 days an increase in density (Fig. 8d, g).

Significant positive correlations were found between the offshore directed across-shore wind (positive wind) and increase of surface density for the inner-mid shelf region (Fig. 8b, e, h). This pattern was stronger during 2012, where high positive correlations extended throughout the upper 500 m (Fig. 8h). During 2010 and 2011, only the upper 200–300 m were influenced by offshore wind pulses (Fig. 8b, e). The alongshore wind component was also correlated with changes in density structure. The negative along-shore wind (from the western to the eastern along Ross Island and from north to south along Victoria Land) was negatively correlated above 200 m with the increase in surface density and a decrease of density below 300 m (Fig. 8c, f, i).

Coherence and phase spectra calculated for across-shore wind and water density at different depths along the inner-mid shelf region in the three years showed significant coherences within the synoptic weather band (4–13 days) above 200 m (Fig. 9). Significant coherences were obtained between offshore wind and density distribution at a 10-day frequency during 2010 above 100 m (Fig. 9a, b) and at 50 and 100 m during 2011, although reduced in magnitude (Fig. 9c, d). During 2012, this same pattern was observed at higher frequencies (4 and 6 days) (Fig. 9e, f). Wind variability leads density variability by 4–6 days (Fig. 9b, d, f). Significant coherences were also observed at higher frequencies (~ 0.25–0.32 cpd, 3.1–4 days), during 2011 and 2012.

The Wedderburn number (equation (2)) provides a measure of the interaction of wind events, with scales of 5–10 days, with the summer stratification for the Victoria Land and Ross Island inner-shelf regions (Fig. 10). These regions were most sampled by the seals and provide a representation of the higher frequency variability present during summer and early fall when the strongest wind events were observed. Winds in excess of $9\,m\,s^{-1}$ and $11\,m\,s^{-1}$ are required to mix across the pycnocline (Wedderburn number < 1) and erode the summer stratification observed for the Ross Island (Fig. 10a) and Victoria Land (Fig. 10b) regions, respectively, in 2010 and 2011. Stratification was stronger in the Victoria Land region ($\Delta\rho = 1.5\,kg\,m^{-3}$) relative to the Ross Island region ($\Delta\rho = 1.1\,kg\,m^{-3}$), requiring stronger winds to mix the water column. The estimated mixed layer depth was shallower in 2012 in both regions, and the wind required to erode the summer stratification was 6 and $7\,m\,s^{-1}$ for Ross Island and Victoria Land, respectively.

3.4. Heat content estimates

Heat content of the upper 300 m for the two inner-shelf regions that were most sampled by the seals during 2010 and 2011 shows that the Ross Island region reached maximum heat content earlier than Victoria Land (Fig. 11a, b). During 2012 the heat content maximum occurred in Victoria Land prior to that at Ross Island. The observed sea ice fraction after April in both regions was larger than 0.5 and showed only minor interannual differences (Fig. 11c). The minimum in sea ice fraction occurred in February, but the magnitude of the minimum differed

between years for the two regions.

The Victoria Land region had the largest interannual differences in minimum sea ice fraction. The January 2012 sea ice fraction was comparable with fall and winter values, but rapidly reached a minimum at the end of February (about 0.3). The decrease was consistent with a peak in heat content (Fig. 11b). The sea ice fraction was minimum in mid-January 2011 (< 0.2) and late February 2012.

Ross Island sea ice fraction showed less interannual differences. During 2010 and 2011 the minimum sea ice was reached at the end of February (< 0.2). The 2012 minimum occurred at the end of February, and rapidly increased after the first week of March (Fig. 11c). The minimum sea ice fraction during 2012 was out of phase with the increase in heat content observed during mid-March in Ross Island (Fig. 11a).

The two regions showed interannual differences in total heat content of about 20%, with Victoria Land having the higher heat content. The averaged heat content in both regions was lower (28% in Ross Island and 16% in Victoria Land) in 2011 and heat loss occurred earlier in the season. The largest accumulated heat content occurred in 2012, with heat accumulation persisting later into the summer and heat loss occurring later in the fall.

4. Discussion

4.1. Temperature-salinity characteristics

The T-S diagrams from the inner-mid shelf region allow inferences to be made about the seasonal formation and erosion of thermohaline properties, interannual variability, and dynamical processes (see conceptual diagram, i.e. Fig. 2). The relative contributions of surface heating, sea ice cover extent, and winds in the three years produce a range of responses in T-S properties. The mid-inner shelf was essentially ice free from February to March 2010 and which allowed the AASW present in the fall-winter to undergo heating and freshening from solar radiation and ice melt, respectively, producing warm and fresh AASW typical of summer conditions (Orsi and Wiederwohl, 2009). The strong winds during summer 2010 contributed to uniform T-S properties in the upper ocean over the area sampled by the seals. The fall-winter freeze in 2011 produced cold, saline AASW and converted the nearly freezing AASW to SW (Orsi and Wiederwohl, 2009). Sea ice remained in the inner-mid shelf region the following summer, reducing the period of open water and producing colder surface conditions. The strong alongshore winds during this time contributed to cooling and sea ice formation.

The two branches of AASW present in summer 2011 showed different levels of cooling and are consistent with regions of ice cover (colder branch) and open water (warmer, fresher branch). The two branches of AASW remained distinct in the 2012 fall-winter transition, suggesting regional variability in the rates of conversion of summer conditions to winter conditions. The upper fresher warmer branch of AASW persisted into the winter and the conversion of AASW seen in 2011 did not occur. The two branches of AASW remained during the 2012 summer transition, with both becoming warmer and fresher. The summer AASW in 2012 was the warmest of the three years. The lower AASW branch in 2012 was similar to the upper branch that formed in 2011 and the single branch in 2010. The different T-S properties of AASW in the three years illustrate the effect of early ice breakup (2010), partial ice coverage (2011) and persistent ice cover into the summer (2012). The differences in AASW properties were reflected in the production of SW, which occurred only in 2011 with partial ice cover and strong winds.

Changes in the inner-mid shelf vertical density structure in the three years showed a progression that is consistent with the T-S diagrams. The general pattern of a lens of low surface density in the summer (produced by ice melt), mixing of less dense water to depth and erosion of stratification in fall-winter (produced by wind, ice formation), and production of more dense water throughout the upper 200 m in winter (produced by ice formation) occurred in each year. However, in 2010 the summer-like stratification of the upper 200 m persisted into the late winter. The early open water in 2010 and extended period of surface heating required more time for the inner-mid shelf to transition to a winter vertical density distribution. In 2011 the summer stratification was reduced, reflecting the persistence of partial ice cover into the summer and higher winds, and the transition to winter conditions occurred in June-July. In 2012 stratification was shallower and was eroded sooner. This year had the densest winter water at the end of winter. The 2011 stratification was intermediate between the fresher deeper conditions in 2010 and the shallow denser conditions in 2012. This progression suggests that it took two years for the mid-inner shelf to adjust from the 2010 conditions to the more typical conditions in 2012.

The thermohaline properties at smaller regional scales can be modified by inputs of water with differing characteristics. For example, advective inputs from other regions could account for the observed heat content changes of the upper water column in the Ross Island region in 2012. Stern et al. (2013) showed that a warm signature observed in McMurdo Sound originated west of the Ross Sea polynya, and was produced by solar heating following ice-free conditions in the polynya. This warmer, fresher and therefore less dense surface water flowed west along the western Ross Ice Shelf font creating a coastal current along the north side of Ross Island and into McMurdo Sound (Robinson et al., 2010).

Observational and modeling studies show that mCDW intrudes onto the Ross Sea continental shelf below 200 m at specific sites that are associated with troughs and shallow banks (Dinniman et al., 2003; Orsi and Wiederwohl, 2009; Kohut et al., 2013). The seal-derived observations from 2012 showed this water mass intruding onto the shelf along Joides Trough (Fig. 5) and extending to the mid-inner-shelf region. The mCDW mixes with the near freezing SW to produce mSW (Orsi and Wiederwohl, 2009). The latter water mass was observed in the T-S distributions from the Victoria Land and Ross Sea regions in fall and winter, highlighting the linkage between onshelf intrusions of mCDW and the inner shelf of the Ross Sea. The seal-derived across-shelf temperature sections show that mCDW reaches the inner shelf where it provides heat to the continental shelf waters and underneath the Ross Ice Shelf. Modeling studies suggest that this input of mCDW contributes to the basal melt rate of the Ross Ice Shelf (Dinniman et al., 2011; Stern et al., 2013).

4.2. Wind forcing and stratification

The ERA-Interim winds used in the correlation analysis accurately represent temporal variability but underestimate maximum wind speeds by about 25%, based on a comparison between shipboard observations and modeled winds (Mack, 2017; Mack et al., 2017). The significant cross-correlations between wind and upper ocean density and across-shore winds and surface density in the Victoria Land and Ross Island regions, depend on the timing of wind events and therefore, represent upper ocean responses to wind forcing (see conceptual diagram). Surface winds in the inner portion of the Ross Sea result from katabatic and synoptic wind events (Murphy and Simmonds, 1993; Parish and Cassano, 2001, 2003). Katabatic winds with speeds of 10–25 m s^{-1} occur in the Victoria Land and Ross Island regions (Parish and Bromwich, 1991; Colacino et al., 2000; Parish and Cassano, 2003), with a main wind direction axis that is across the coastline (Colacino et al., 2000). The coastal regions of the western Ross Sea also experience frequent cyclone activity that influences surface winds (Cassano and Parish, 2000). These synoptic scale events occur with a frequency of 3–10 days and are characterized by wind speeds of 15–35 m s^{-1} (Bromwich, 1991; Parish and Cassano, 2003).

Each wind event produces mixing in the upper ocean (< 200 m) that incrementally erodes the surface summer stratification, which is

dominated by a low-density shallow surface mixed layer above a sharp pycnocline. Entrainment of high-density water in the surface layer occurs during the summer-fall-winter progression of the upper ocean. The observed interannual variability in the erosion of the seasonal stratification is related to the frequency and strength of the wind events. Even with underestimation of the strength of the ERA-Interim winds, there is a clear correspondence between wind events and stratification. The more stratified inner shelf during 2012 was associated with less intense wind events ($\sim < 5\,m\,s^{-1}$); strong ($> 6–10\,m\,s^{-1}$) wind pulses destratified the water column earlier during 2010 and 2011. The implication is that erosion of the seasonal stratification is an incremental process that is moderated by the frequency of wind events with speeds above a particular threshold. However, the wind speeds associated with destratification should be taken as a guide because regions of the inner Ross Sea continental shelf are covered with fast ice, which modifies the effective wind stress.

4.3. Heat content

The seal-derived temperature measurements provided the first characterization of seasonal and interannual variability in upper ocean heat content for the inner-shelf region of the western Ross Sea. The heat loss expected from seasonal cooling is influenced by strong wind events, such as the one in early March 2010 for the Ross Island region and the one in late February-early March 2011 for the Victoria Land region. The persistence of heat in the upper water column into late March 2012 in both regions coincided with an extended period of weaker winds.

The evolution of the heat content for the inner part of the Ross Sea can be compared to that calculated for the western Antarctic Peninsula (WAP), also based on temperature time series obtained from seal-derived measurements (Costa et al., 2008). The integrated heat content for the upper 200 m for the inner-shelf regions of the Ross Sea is about 50% of the heat content along the WAP and reaches its minimum value about 2.5 months earlier. These differences are consistent with the higher latitude and the colder form of mCDW that occurs in the Ross Sea. The winter heat content of the Ross Sea is near zero whereas that of WAP continental shelf waters remains around 50% of the late fall value. The implication is that the water column in the inner Ross Sea is essentially well mixed throughout the upper 300 m in winter as a result of convection, as shown in other parts of the western Ross Sea (e.g. Gordon et al., 2000). Winter mixing on the WAP continental shelf is shallower (Prézelin et al., 2004) and mixes warm mCDW (1–1.5 °C) into the upper water column (Klinck et al., 2004), thereby providing a continual source of heat. The quantitative comparisons of seasonal differences in heat content properties of the Ross Sea and WAP regions provided by the seal-collected measurements highlight the differences in cold (limited influence of CDW) versus warm (strongly influenced by CDW) Antarctic continental shelves.

4.4. Implications for the future state of the western Ross Sea

The Ross Sea is experiencing changes in atmospheric conditions. Cold southerly winds blowing seaward from the Ross Ice Shelf have strengthened (Turner et al., 2009; Smith et al., 2014), potentially increasing vertical mixing. However, projections of future winds over the Ross Sea suggest slight weakening of the westerly component relative to current conditions (Bracegirdle et al., 2013). Modeling studies of the effects of these projected changes (Smith et al., 2014) suggest that by 2100 winds near the Victoria Land coast will be weaker, while winds will be stronger near the continental shelf break. As a result, mean summer mixed layer depths will decrease, and the duration of shallow mixed layers over the continental shelf will increase. Other potential changes by 2100 include a summer expansion of the Ross Sea polynya, which will increase heat to the upper ocean and also support an extended phytoplankton growing season (Smith et al., 2014). Expansion of the Ross Sea polynya will modify inputs of less dense surface waters that form along the inner shelf of the western Ross Ice Shelf (Stern et al., 2013; Arzeno et al., 2014) and flow into the Ross Island region. Increased inputs of surface fresh water will require stronger winds to erode the enhanced stratification.

A reduction in wind strength over the next century may contribute to a more stratified coastal ocean. This analysis shows that a threshold exists for wind events with speeds sufficient to breakdown stratification. This wind speed threshold may increase should the Ross Sea continue to freshen (Smith et al., 2014; Dinniman et al., 2017). Weakened winds may still have synoptic scale events that exceed this threshold, but the number and frequency of these is unknown. Seal-derived hydrographic measurements are adequate for providing realizations of the ocean state, but these measurements need to be combined with simultaneous atmosphere measurements to adequately describe changes.

The projected changes in the atmospheric conditions have important consequences for the thermohaline and sea ice properties of the coastal ocean along the inner shelf of the western Ross Sea. The use of seals as platforms to measure and monitor the hydrography of the Ross Sea will allow near synoptic views of environmental changes that can also be related to changes in seal ecology, behavior, and habitat use. The ability to measure evolving environmental conditions and processes provides a strong constraint for implementing and evaluating circulation and ecological models designed to assess responses to projected changes in the Ross Sea.

Acknowledgments

This study was supported by the National Science Foundation Grants ANT-0944174 (to EEH, JMK, MSD), ANT-0838911 (to EEH), ANT-0838892 (to DCP), and ANT-0838937 (to JMB). The U.S. National Science Foundation through the U.S. Antarctic Program provided logistical support for this project in Antarctica. A. Piñones also acknowledges support from CONICYT/Chile through the Program FONDAP, Project 15150003 and PAI Project 79160077. JMB contributed to this work while serving at the National Science Foundation. Any opinion, findings, and conclusions or recommendations expressed in this material are those of the author(s) and do not necessarily reflect the views of the National Science Foundation. We thank Laurie Padman and one anonymous reviewer for insightful and helpful comments and suggestions on an earlier and this version of this manuscript.

Appendix A. Supplementary material

Supplementary data to this article can be found online at https://doi.org/10.1016/j.pocean.2019.01.003.

References

Arzeno, I.B., Beardsley, R.C., Limeburner, R., Owens, B., Padman, L., Springer, S.R., Stewart, C.L., Williams, M.J.M., 2014. Ocean variability contributing to basal melt rate near the ice front of Ross Ice Shelf, Antarctica. J. Geophys. Res. Oceans 119, 4214–4233. https://doi.org/10.1002/2014JC009792.

Biuw, M., Boehme, L., Guinet, C., Hindell, M., Costa, D., Charrassin, J.B., Roquet, F., Bailleul, F., Meredith, M., Thorpe, S., Tremblay, Y., McDonald, B., Park, Y.H., Rintoul, S.R., Bindoff, N., Goebel, M., Crocker, D., Lovell, P., Nicholson, J., Monks, F., Fedak, M.A., 2007. Variations in behaviour and condition of a Southern Ocean top predator in relation to in situ oceanographic conditions. Proc. Natl. Acad. Sci. USA 104, 13705–13710.

Boehme, L., Lovell, P., Biuw, M., Roquet, F., Nicholson, J., Thorpe, S.E., Meredith, M.P., Fedak, M., 2009. Technical note: animal-borne CTD-satellite relay data loggers for real-time oceanographic data collection. Ocean Sci. 5, 685–695.

Bost, C.A., Cotté, C., Bailleul, F., Cherel, Y., Charrassin, J.B., Guinet, C., Ainley, D.G., Weimerskirch, H., 2009. The importance of oceanographic fronts to marine birds and mammals of the southern oceans. J. Mar. Syst. 78, 363–376.

Bost, C.A., Cotte, C., Terray, P., Barbraud, C., Bon, C., Delord, K., Gimenez, O., Handrich, Y., Naito, Y., Guinet, C., Weimerskirch, H., 2015. Large-scale climatic anomalies affect marine predator foraging behaviour and demography. Nat. Commun. 6, 8220.

Bracegirdle, T.J., Shuckburgh, E., Salleé, J.-B., Wang, Z., Meijers, A.J.S., Bruneau, N., Phillips, T., Wilcox, L.J., 2013. Assessment of surface winds over the Atlantic, Indian, and Pacific Ocean sectors of the Southern Ocean in CMIP5 models: historical bias,

forcing response, and state dependence. J. Geophys. Res. Atmos. 118, 547–562. https://doi.org/10.1002/jgrd.50153.
Bromwich, D.H., 1991. Mesoscale cyclogenesis over the southwestern Ross Sea linked to strong katabatic winds. Mon. Weather Rev. 119, 1736–1752.
Budillon, G., Castagno, P., Aliani, S., Spezie, G., Padman, L., 2011. Thermohaline variability and Antarctic bottom water formation at the Ross Sea shelf break. Deep-Sea Res. 58 (10), 1002–1018. https://doi.org/10.1016/j.dsr.2011.07.002.
Burns, J.M., Castellini, M.A., Testa, J.W., 1999. Movements and diving behaviour of weaned Weddell seal (*Leptonychotes weddellii*) pups. Polar Biol. 21, 23–36.
Burns, J.M., Kooyman, G.L., 2001. Habitat use by Weddell Seals and Emperor Penguins in the Ross Sea, Antarctica. Am. Zool. 41, 90–98.
Castellini, M.A., Davis, R.W., Kooyman, G.L., 1992. Annual cycles of diving behavior and ecology of the Weddell seal. Bull. Scripps Inst. Oceanogr. 28, 1–54.
Cassano, J.J., Parish, T.R., 2000. An analysis of nonhydrostatic dynamics in numerically simulated Antarctic katabatic flows. J. Atmos. Sci. 57, 891–898.
Charrassin, J.-B., Hindell, M., Rintoul, S.R., Roquet, F., Sokolov, S., Biuw, M., Costa, D., Boehme, L., Lovell, P., Coleman, R., Timmermann, R., Meijers, A., Meredith, M., Park, Y.-H., Bailleul, F., Goebel, M., Tremblay, Y., Bost, C.-A., McMahon, C.R., Field, I.C., Fedak, M.A., Guinet, C., 2008. Southern Ocean frontal structure and sea-ice formation rates revealed by elephant seals. Proc. Natl. Acad. Sci. 105, 11634–11639.
Colacino, M., Piervitali, E., Grigioni, P., 2000. Climatic characterization of the Terra Nova Bay Region. In: Faranda, F.M., Guglielmo, L., Ionora, A. (Eds.), Ross Sea Ecology. Springer-Verlag, Berlin, pp. 15–26.
Comiso, J.C., Kwok, R., Martin, S., Gordon, A.L., 2011. Variability and trends in sea ice extent and ice production in the Ross Sea. J. Geophys. Res. 116, C04021. https://doi.org/10.1029/2010JC006391.
Comiso, J.C., 2010. Polar Oceans from Space. Springer, New York 507pp.
Comiso, J.C., Gertsen, R.A., Stock, L.V., Turner, J., Perez, G.J., Cho, K., 2017. Positive trend in the Antarctic sea ice cover and associated changes in surface temperature. J. Clim. 30, 2251–2267. https://doi.org/10.1175/JCLI-D-16-0408.1.
Costa, D.P., Klinck, J.M., Hofmann, E.E., Dinniman, M.S., Burns, J.M., 2008. Upper ocean variability in west Antarctic Peninsula continental shelf waters as measured using instrumented seals. Deep-Sea Res. II 55, 323–337.
Costa, D.P., Breed, G.A., Robinson, P.W., 2012. New insights into pelagic migrations: implications for ecology and conservation. Annu. Rev. Ecol. Evol. Syst. 43, 73–96.
Dee, D.P., et al., 2011. The ERA-Interim reanalysis: configuration and performance of the data assimilation system. Quart. J. R. Meteorol. Soc. 137, 553–597. https://doi.org/10.1002/qj.828.
Dinniman, M.S., Klinck, J.M., Smith Jr., W.O., 2003. Cross-shelf exchange in a model of the Ross Sea circulation and biogeochemistry. Deep Sea Res. II 50, 3103–3120.
Dinniman, M.S., Klinck, J.M., Smith Jr., W.O., 2011. A model study of Circumpolar Deep Water on the west Antarctic Peninsula and Ross Sea continental shelves. Deep-Sea Res. II 58, 1508–1523. https://doi.org/10.1016/j.dsr2. 2010.11.013.
Dinniman, M.S., Klinck, J.M., Hofmann, E.E., Smith Jr., W.O., 2017. Effects of projected changes in wind, atmospheric temperature, and freshwater inflow on the Ross Sea. J. Clim. https://doi.org/10.1175/JCLI-D-17-0351.1.
Emery, W.J., Thomson, R.E., 1998. Data Analysis Methods in Physical Oceanography. Pergamon, New York, pp. 480–495.
Fedak, M.A., Lovell, P., Grant, S.M., 2001. Two approaches to compressing and interpreting time-depth information as collected by time-depth recorders and satellite-linked data recorders. Mar. Mammal Sci. 17, 94–110.
Fedak, M., Lovell, P., McConnell, B., Hunter, C., 2002. Overcoming constraints of long range radio telemetry from animals: getting more useful data from smaller packages. Integr. Comp. Biol. 42, 3–10.
Fedak, M.A., 2013. The impact of animal platforms on polar ocean observation. Deep Sea Res. Part II 88–89, 7–13.
Goetz, K.T., 2015. Movement, habitat, and foraging behavior of Weddell seals (Leptonychotes weddellii) in the western Ross Sea, Antarctica. PhD Dissertation. University of California Santa Cruz, p. 155.
Gordon, L.I., Codispoti, L.A., Jennings Jr., J.C., Millero, F.J., Morrison, J.M., Sweeney, C., 2000. Seasonal evolution of hydrographic properties in the Ross Sea, Antarctica, 1996–1997. Deep Sea Res., Part II 47 (15–16), 3095–3117.
Gordon, A.L., Orsi, A.H., Muench, R., Huber, B.A., Zambianchi, E., Visbeck, M., 2009. Western Ross Sea continental slope gravity currents. Deep-Sea Res. II 56, 796–817.
Gordon, A.L., Huber, B.A., Busecke, J., 2015. Bottom water export from the western Ross Sea, 2007 through 2010. Geophys. Res. Lett. 42, 5387–5394. https://doi.org/10.1002/2015GL064457.
Holland, P.R., Kwok, R., 2012. Wind-driven trends in Antarctic sea-ice drift. Nat. Geosci. 5, 872–875.
Imberger, J., 1985. The diurnal mixed layer. Limnol. Oceanogr. 30, 737–770.
Kaufman, D.E., Friedrichs, M.A.M., Smith Jr., W.O., Queste, B.Y., Heywood, K.J., 2014. Biogeochemical variability in the southern Ross Sea as observed by a glider deployment. Deep-Sea Res. I 92, 93–106.
Klinck, J.M., Hofmann, E.E., Beardsley, R.C., Salihoglu, B., Howard, S., 2004. Water mass properties and circulation on the west Antarctic Peninsula continental shelf in austral fall and winter 2001. Deep-Sea Res. II 51, 1925–1946.
Kohut, J., Hunter, E., Huber, B., 2013. Small-scale variability of the cross-shelf flow over the outer shelf of the Ross Sea. J. Geophys. Res. Oceans 118, 1863–1876.
Mack, S.L., 2017. Influence of tides and mesoscale eddies in the Ross Sea. PhD Dissertation. Old Dominion University, pp. 146.
Mack, S.L., Dinniman, M.S., McGillicuddy Jr., D.J., Sedwick, P.N., Klinck, J.M., 2017. Dissolved iron transport pathways in the Ross Sea: influence of tides and mesoscale eddies in a regional ocean model. J. Mar. Syst. 166, 73–86.
Murphy, B.F., Simmonds, I., 1993. An analysis of strong wind events simulated in a GCM near Casey in the Antarctic. Mon. Weather Rev. 121, 522–534.
Orsi, A.H., Johnson, G.C., Bullister, J.L., 1999. Circulation, mixing, and production of Antarctic Bottom Water. Prog. Oceanogr. 43, 55–109.
Orsi, A.H., Wiederwohl, C.L., 2009. A recount of Ross Sea waters. Deep-Sea Res. II 56, 778–795. https://doi.org/10.1016/j.dsr2.2008.10.033.
Parish, T.R., Bromwich, D.H., 1991. Continental-scale simulation of the Antarctic katabatic wind regime. J. Clim. 4 (2), 135–146.
Parish, T.R., Cassano, J.J., 2001. Forcing of the wintertime Antarctic boundary layer winds from the NCEP/NCAR global reanalysis. J. Appl. Meteorol. 40, 810–821.
Parish, T.R., Cassano, J.J., 2003. The role of katabatic winds on the Antarctic surface wind regime. Mon. Weather Rev. 131, 317–333.
Parkinson, C.L., 2002. Trends in the length of the Southern Ocean sea-ice season. Ann. Glaciol. 34, 435–440. https://doi.org/10.3189/172756402781817482.
Prézelin, B.B., Hofmann, E.E., Moline, M., Klinck, J.M., 2004. Physical forcing of phytoplankton community structure and primary production in continental shelf waters of the western Antarctic Peninsula. J. Mar. Res. 62, 419–460.
Robinson, N.J., Williams, M.J.M., Barrett, P.J., Pyne, A.R., 2010. Observations of flow and ice-ocean interaction beneath the McMurdo Ice Shelf, Antarctica. J. Geophys. Res. 115, C03025. https://doi.org/10.1029/2008JC005255.
Roquet, F., Park, Y.-H., Guinet, C., Bailleul, F., Charrassin, J.-B., 2009. Observations of the Fawn Trough Current over the Kerguelen Plateau from instrumented elephant seals. J. Mar. Syst. 78, 377–393.
Roquet, F., Charrassin, J.-B., Marchand, S., Boehme, L., Fedak, M., Reverdin, G., Guinet, C., 2011. Delayed-mode calibration of hydrographic data obtained from animal-borne satellite relay data loggers. J. Atmos. Ocean. Technol. 28, 787–801.
Roquet, F., Wunsch, C., Forget, G., Heimbach, P., Guinet, C., Reverdin, G., Charrassin, J.-B., Bailleul, F., Costa, D.P., Huckstadt, L.A., Goetz, K.T., Kovacs, K.M., Lydersen, C., Biuw, M., Nøst, O.A., Bornemann, H., Ploetz, J., Bester, M.N., McIntyre, T., Muelbert, M.C., Hindell, M.A., McMahon, C.R., Williams, G., Harcourt, R., Field, I.C., Chafik, L., Nicholls, K.W., Boehme, L., Fedak, M.A., 2013. Estimates of the Southern Ocean general circulation improved by animal-borne instruments. Geophys. Res. Lett. 40, 6176–6180.
Roquet, F., Williams, G., Hindell, M.A., Harcourt, R., McMahon, C., Guinet, C., Charrassin, J.-B., Reverdin, G., Boehme, L., Lovell, P., Fedak, M., 2014. A Southern Indian Ocean database of hydrographic profiles obtained with instrumented elephant seals. Nat. Sci. Data 1, 140028.
Rual, P., 1996. Onboard quality control of XBT bathy messages. Intergovernmental Oceanographic Commission of UNESCO and World Meteorological Organization Report IOC/INF-1021: Summary of ship-of-opportunity programmes and technical reports. Paris, 25 January 1996, pp. 142–152.
Smith Jr., W.O., Asper, V., Tozzi, S., Liu, X., Stammerjohn, S.E., 2011. Surface layer variability in the Ross Sea, Antarctica as assessed by in situ fluorescence measurements. Prog. Oceanogr. 88, 28–45. https://doi.org/10.1016/j.pocean.2010.08.002.
Smith Jr., W.O., Dinniman, M.S., Hoffman, E.E., Klinck, J., 2014. The effects of changing winds and temperatures on the oceanography of the Ross Sea in the 21st century. Geophys. Res. Lett. 41, 1624–1631. https://doi.org/10.1002/2014GL059311.
Stammerjohn, S.E., Martinson, D.G., Smith, R.C., Yuan, X., Rind, D., 2008. Trends in Antarctic annual sea ice retreat and advance and their relation to ENSO and Southern Annular Mode variability. J. Geophys. Res. 113, C03S90. https://doi.org/10.1029/2007JC004269.
Stammerjohn, S.E., Maksym, T., Heil, P., Massom, R.A., Vancoppenolle, M., Leonard, K.C., 2011. The influence of winds, sea-surface temperature and precipitation anomalies on Antarctic regional sea-ice conditions during IPY 2007. Deep Sea Res. II 58, 999–1018. https://doi.org/10.1016/j.dsr2.2010.10.026.
Stern, A.A., Dinniman, M.S., Zagorodnov, V., Tyler, S.W., Holland, D.M., 2013. Intrusion of warm surface water beneath the McMurdo Ice Shelf Antarctica. J. Geophys. Res. 118, 7036–7048. https://doi.org/10.1002/2013JC008842.
Testa, J.W., 1994. Over-winter movements and diving behavior of female Weddell seals (*Leptonychotes weddellii*) in the southwestern Ross Sea, Antarctica. Can. J. Zool. 72, 1700–1710.
Turner, J., Comiso, J.C., Marshall, G.J., Connolley, W.M., Lachlan-Cope, T.A., Bracegirdle, T., Wang, Z., Meredith, M., Maksym, T., 2009. Antarctic sea ice extent increases as a result of anthropogenic activity. Geophys. Res. Lett. 36, L08502. https://doi.org/10.1029/2009GL037524.
Turner, J., Hosking, J.S., Marshall, G.J., Phillips, T., Bracegirdle, T.J., 2016. Antarctic sea ice increase consistent with intrinsic variability of the Amundsen Sea Low. Climate Dyn. 46, 2391–2402. https://doi.org/10.1007/s00382-015-2708-9.